

Short communication

# Highly-optimized membrane electrode assembly for direct methanol fuel cell prepared by sedimentation method

Jing Hua Liu, Min Ku Jeon, Won Choon Choi, Seong Ihl Woo\*

*Department of Chemical & Biomolecular Engineering, Korea Advanced Institute of Science and Technology, 373-1, Kusong-Dong, Yusong-gu, Taejeon 305-701, South Korea*

Received 19 March 2004; accepted 28 May 2004

Available online 12 August 2004

## Abstract

An electrode for a direct methanol fuel cell (DMFC) is prepared by means of the sedimentation method. A suspension containing Pt black, PTFE and water was filtered through a polycarbonate film and a thin catalyst layer remains on this film. This catalyst layer is then transferred to a gas-diffusion layer by applying a pressure to the assembly and then peeling off the filter film. For the anode catalyst layer, the suspension contained Pt–Ru black and water. The preparation process is optimized and single-cell performance is examined under different operating conditions. Operated at 60 °C, the output power density of the membrane electrode assembly (MEA) fabricated by the sedimentation method is 70% higher than that for an assembly prepared by the conventional brushing technique.

© 2004 Elsevier B.V. All rights reserved.

**Keywords:** Sedimentation method; Direct methanol fuel cell; Membrane electrode assembly; Power density

## 1. Introduction

The direct methanol fuel cell (DMFC) is attracting attention due to its flexibility of application [1–10]. The efficiency of the DMFC must be improved, however, for commercial realization to be achieved. This requires finding more active electrodes, decreasing methanol cross over, and by devising a more effective membrane electrode assembly (MEA) [11]. While extensive research has been conducted on MEAs for hydrogen–oxygen proton-exchange fuel cells (PEMFCs), fewer studies of MEAs for DMFCs have been reported. The methods of fabricating MEAs for H<sub>2</sub>–O<sub>2</sub> PEMFCs include a brushing method [12], a doctor-blade technique [13], screen printing [14,15], rolling method [16–18], a spraying method [19,20], and a decal method [21]. The requirements for the electrode structure of a DMFC are quite different, however,

than those for a H<sub>2</sub>–O<sub>2</sub> PEMFC. The electrode of the DMFC usually contains more platinum, sometimes ten times higher, than that of H<sub>2</sub>–O<sub>2</sub> PEMFC because of the low activity of methanol electrooxidation [22] and the crossover of methanol to the cathode side [23–25] in the case of a liquid-fed DMFC. Thus, the thickness of the catalyst layer of the DMFC electrode is much higher than that of the H<sub>2</sub>–O<sub>2</sub> PEMFC electrode. When conventional methods are used to fabricate the DMFC anode, it is difficult to produce a perfectly homogeneous catalyst layer due to the fact that large systematic errors exist in the preparation process.

In this study, a DMFC electrode is fabricated using the sedimentation method in which the manual work is reduced to a minimum. A planar and homogeneous catalyst layer is obtained. The systematic errors are reduced and thus good reproducibility is achieved. Several parameters in the manufacturing of the electrode are optimized and the resulting performance of the resulting electrode is compared with that prepared by the conventional brushing method.

\* Corresponding author. Tel.: +82 42 869 8899; fax: +82 42 869 8890.  
E-mail address: [siwoo@mail.kaist.ac.kr](mailto:siwoo@mail.kaist.ac.kr) (S.I. Woo).

## 2. Experimental

### 2.1. Fabrication of membrane electrode assemblies (MEA) by sedimentation method

The substrate for the catalyst layer was wet-proofed Toray carbon paper with a gas-diffusion layer. The gas-diffusion layer for the cathode and for the anode comprised XC-72 carbon and 20 wt.% PTFE, and XC-72 carbon and 7 wt.% of Nafion ionomer, respectively. Pt and Pt–Ru black (Johnson Matthey Co.) were used as the cathode and anode catalyst, respectively. The electrode preparation method reported by Sun et al. [26] was modified and the sedimentation method for fabricating the electrode is as follows.

The catalyst powder was suspended in water in an ultrasonic bath until a homogeneous ink was formed. Using a vacuum-filtering device, the suspension was filtered through a polycarbonate filter film that had an average pore size of 1  $\mu\text{m}$  and thus an even and planar layer of catalyst remained on one side of the filter film. The catalyst-loaded filter film was then removed from the filtering device and a thin layer of glycerol was applied to the backside of the film. The catalyst layer was then transferred from the filter film to the gas-diffusion layer by compacting the assembly with a hydraulic press, and then the polycarbonate filter film was peeled off. The resulting electrode was vacuum dried at 110  $^{\circ}\text{C}$  for 24 h. A Nafion 115 membrane was treated with 3%  $\text{H}_2\text{O}_2$  and 0.5 M  $\text{H}_2\text{SO}_4$  and then sandwiched between the prepared anode and cathode assembly. The assembly was hot pressed at 130  $^{\circ}\text{C}$  for 90 s under a pressure of 100 atm. The Pt–Ru and Pt loadings of both the anode and the cathode were 5  $\text{mg cm}^{-2}$ .

### 2.2. Single-cell test

Polarization curves were obtained using a single cell with a working area of 4  $\text{cm}^2$ . Unless otherwise specified, Pt–Ru and Pt blacks were used as the anode and cathode catalysts, respectively. The MEA was sandwiched between two graphite plates with straight channel flow-fields. Two pieces of rubber gasket were used to seal the MEA. The single cell was heated to the required temperature by two electrical heaters attached to the outer surface of the end plates. 2 M aqueous methanol solution was fed to the anode side using a peristaltic pump at a flow rate of 2  $\text{ml min}^{-1}$ . Oxygen was supplied to the cathode chamber under ambient pressure.

## 3. Results and discussion

### 3.1. Comparison of power densities of MEAs prepared by sedimentation and brushing methods

The power density curves of a single cell operated at various temperatures are presented in Fig. 1. Peak values of the power densities appear at a cell voltage ( $E_c$ ) of 0.4 V. In Table 1, a comparison of power densities is made between

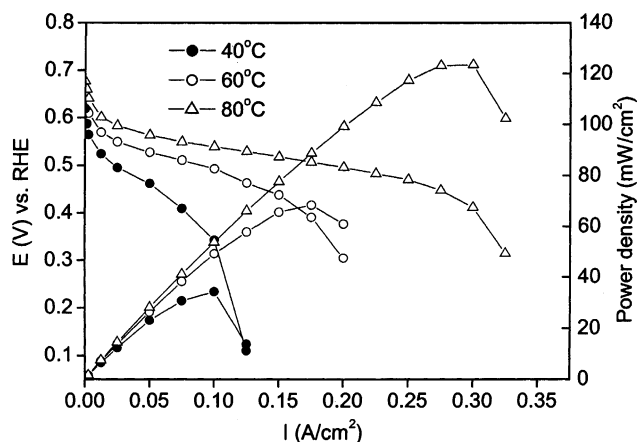


Fig. 1. Power density curves for single cell at various temperatures. Pt and Pt–Ru loading: 5  $\text{mg cm}^{-2}$ ;  $P_{\text{O}_2}$ : ambient pressure;  $\text{O}_2$  flow rate = 500  $\text{ml min}^{-1}$ ;  $\text{CH}_3\text{OH}$ : 2.0 M;  $\text{CH}_3\text{OH}$  flow rate = 2  $\text{ml min}^{-1}$ .

the MEA fabricated by a sedimentation method and that by the conventional brushing method. At a cell temperature of 40  $^{\circ}\text{C}$ , the power density of MEA prepared by the sedimentation method is only 10% higher than that by the brushing method. At higher temperatures of 60 and 80  $^{\circ}\text{C}$ , the power densities of the MEA prepared by sedimentation method are 70 and 180% higher than those prepared by the brushing method, respectively.

As noted above, various methods have been developed to prepare electrode for  $\text{H}_2$ – $\text{O}_2$  PEMFCs and, DMFC. There are common disadvantages with these methods, namely, the requirement for skilled hands and the inevitable large systematic errors. Therefore, a fabrication method without the influence of manual work is required. Using the sedimentation method developed in this study, the catalyst layer is formed under the force of gravity and vacuum suction. As a result, a very homogenous and planar catalyst layer can be produced with the least systematic errors. In addition, the diffusion of methanol, whose molecular size is larger than hydrogen, into the catalyst layer and the removal of carbon dioxide away from the catalytic sites require a DMFC anode with an ‘open’ structure [27]. During the sedimentation process, a perpendicularly-oriented network of pores in the catalyst layer is generated through the spontaneous accumulation of the catalyst particles and the filtering process, which facilitates the mass transport of both reactants and the products.

Table 1  
Comparison of power densities ( $\text{mW cm}^{-2}$ ) of a MEA fabricated by a sedimentation or brushing method operated at a cell voltage of 0.4 V

	40 $^{\circ}\text{C}$	60 $^{\circ}\text{C}$	80 $^{\circ}\text{C}$
Sedimentation	30	68	123
Brushing	27	40	44

Pt and Pt–Ru loading = 5  $\text{mg cm}^{-2}$ ;  $P_{\text{O}_2}$ : ambient pressure;  $\text{O}_2$  flow rate = 500  $\text{ml min}^{-1}$ ;  $\text{CH}_3\text{OH}$  = 2.0 M;  $\text{CH}_3\text{OH}$  flow rates = 2  $\text{ml min}^{-1}$ .

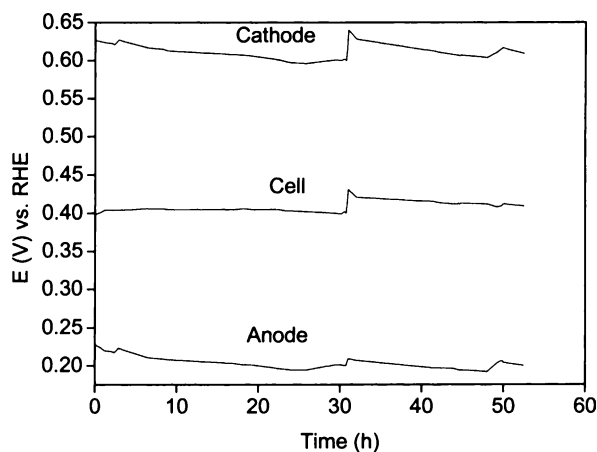


Fig. 2. Durability test of single cell at  $0.16 \text{ A cm}^{-2}$ . Pt and Pt–Ru loading =  $5 \text{ mg cm}^{-2}$ ;  $T = 60^\circ \text{C}$ ;  $P_{\text{O}_2}$ : ambient pressure;  $\text{O}_2$  flow rate =  $500 \text{ ml min}^{-1}$ ;  $\text{CH}_3\text{OH}$ :  $2.0 \text{ M}$ ;  $\text{CH}_3\text{OH}$  flow rate =  $2 \text{ ml min}^{-1}$ .

The results of a durability test of the MEA prepared by the sedimentation method when operated at a constant current density of  $0.16 \text{ A cm}^{-2}$  are given in Fig. 2. The cell voltage increases from  $0.396$  to  $0.406 \text{ V}$  after  $6.33 \text{ h}$  of operation. This behaviour is due to the fact that the Nafion membrane and the Nafion ionomer contained in the catalyst layer are hydrated by the methanol solution fed to the anode side and the water produced at the cathode side. After a future  $24 \text{ h}$  of operation, the cell voltage decreases from  $0.406$  to  $0.4 \text{ V}$ . The degradation in cell voltage is  $0.25 \text{ mV h}^{-1}$ , which is smaller than the  $0.3 \text{ mV h}^{-1}$  reported by Waidhas et al. [28] and the  $2.5 \text{ mV h}^{-1}$  reported by Sukla et al. [29]. Therefore, the MEA prepared by the sedimentation method displays good stability in long-term operation. After  $32 \text{ h}$  of operation, the test was stopped for  $15 \text{ min}$ . During this time, the circulation of methanol solution and the flow of oxygen were continued. When the operation was resumed, the cathode potential ( $\varphi_c$ ), anode potential ( $\varphi_a$ ) and  $E_c$  was  $0.64$ ,  $0.209$  and  $0.431 \text{ V}$ , respectively, which is  $40$ ,  $31$  and  $9 \text{ mV}$  higher than before the rest time. The cathode potential is increased because the excess water produced during the  $32 \text{ h}$  of operation is removed by the oxygen flow during the rest time, which results in a good condition of humidity in the cathode catalyst layer.

### 3.2. Order of adding Nafion to catalyst layer

The order of adding Nafion to the cathode catalyst layer was studied. Two methods were prepared of which one involved dissolving Nafion solution into the catalyst suspension before the sedimentation process and the other involved impregnating Nafion solution after the catalyst layer was fabricated by the sedimentation method. To perform the first method, the amount of Nafion added to the catalyst suspension was calibrated because some portion of Nafion was removed during filtering. In the second method,  $5\%$  Nafion solution was dropped directly onto the horizontal surface of

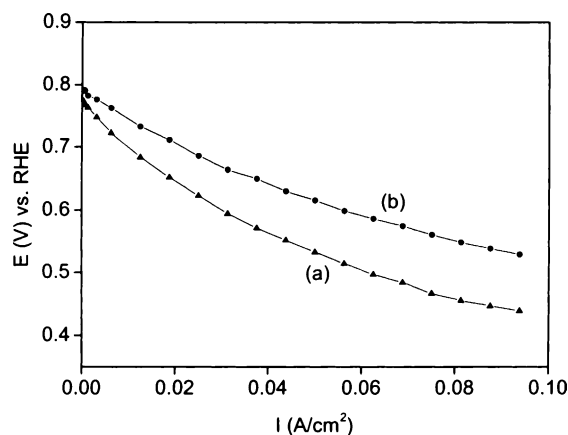


Fig. 3. Comparison of methods of adding Nafion to cathode catalyst layer, (a) Nafion added to catalyst suspension before sedimentation process; (b) impregnation of the Nafion into a catalyst layer prepared by sedimentation method Pt loading =  $5 \text{ mg cm}^{-2}$   $T = 28^\circ \text{C}$ ;  $P_{\text{O}_2}$ : ambient pressure;  $\text{O}_2$  flow rate =  $500 \text{ ml min}^{-1}$ ; electrolyte =  $2.0 \text{ M H}_2\text{SO}_4 + 2.0 \text{ M CH}_3\text{OH}$ ; electrolyte flow rate =  $2 \text{ ml min}^{-1}$ .

the catalyst layer and dried in air under ambient temperature. The Nafion loadings of both methods were  $20 \text{ wt.}\%$ . As shown in Fig. 3, the cathode gave better performance with the second method than with the first. When Nafion is homogeneously mixed with the catalyst, some portion of pores in the catalyst layer is blocked by the Nafion ionomer after the electrode is prepared by the sedimentation method. Consequently, there are not sufficient passages for the reactant agents to access the active sites of the catalyst particles. Furthermore, Nafion ionomer remains between some catalyst particles and thus prevents electronic conduction between these particles, as shown in Fig. 4. When using the impregnation method, Nafion solution flows through the network of pores in the catalyst layer in a direction perpendicular to the surface of the electrode and does not block the pores that are situated far from the outer surface of the catalyst layer. Thus, there exists sufficient diffusion pathways for the reactant agents. Electronic conduction among the catalyst particles is not affected by the impregnation of Nafion. Furthermore, a very thin layer of Nafion forms on the surface of the catalyst layer and improves the bonding between the catalyst layer and the Nafion membrane after the hot-pressing process.

### 3.3. Optimized amount of PTFE

The effect of PTFE content on the cathode performance was studied. The emulsion of PTFE was added into the catalyst suspension and then the catalyst layer containing PTFE was prepared by the sedimentation method. The amount of residual PTFE in the prepared catalyst layer was also calibrated and an accurate amount of PTFE was added to the catalyst suspension. Experiments optimizing the content of PTFE were carried out in a half-cell, in which the electrolyte was  $2 \text{ M H}_2\text{SO}_4$  or  $2 \text{ M H}_2\text{SO}_4 + 2 \text{ M CH}_3\text{OH}$ . As shown

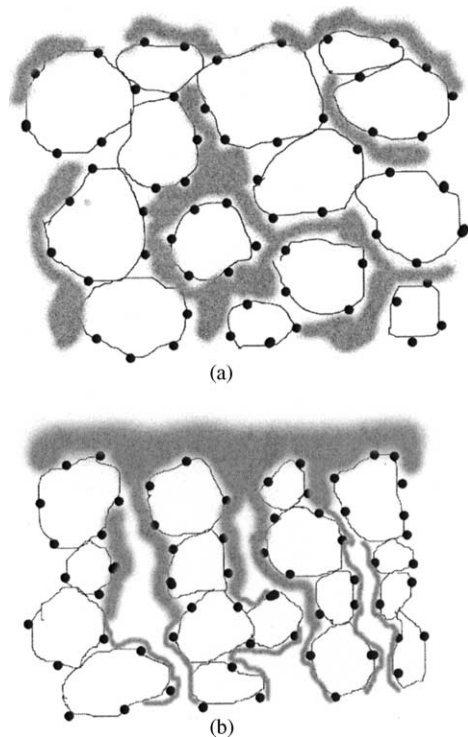


Fig. 4. Schematic of Nafion distribution in fee catalyst layer, (a) Nafion added to catalyst suspension before sedimentation process; (b) impregnation Nafion into catalyst layer prepared by sedimentation method.

in Fig. 5, a cathode containing 15 wt.% PTFE in the catalyst layer shows better performance than one that without PTFE when 2 M H<sub>2</sub>SO<sub>4</sub> was used as the electrolyte at 28 °C. The cathode containing 30 wt.% PTFE exhibits the worst performance. When 15 wt.% PTFE is added to the catalyst layer, an optimum network of pores in the catalyst layer is formed due to the hydrophobic property of PTFE, which makes the mass transport of oxygen and water more efficient without flooding. As the PTFE content is raised further to 30 wt.%, the insulation effect of PTFE increases the inner resistance

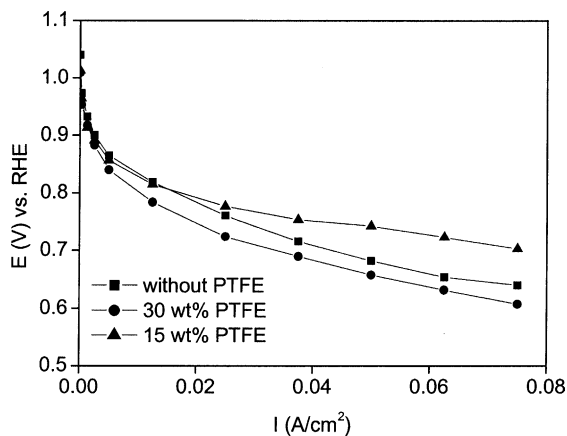


Fig. 5. Effect of PTFE content on cathode performance. Pt loading = 5 mg cm<sup>-2</sup> T = 28 °C; P<sub>O<sub>2</sub></sub>: ambient pressure; O<sub>2</sub> flow rate = 500 ml min<sup>-1</sup>; electrolyte = 2.0 M H<sub>2</sub>SO<sub>4</sub>; electrolyte flow rate = 2 ml min<sup>-1</sup>.

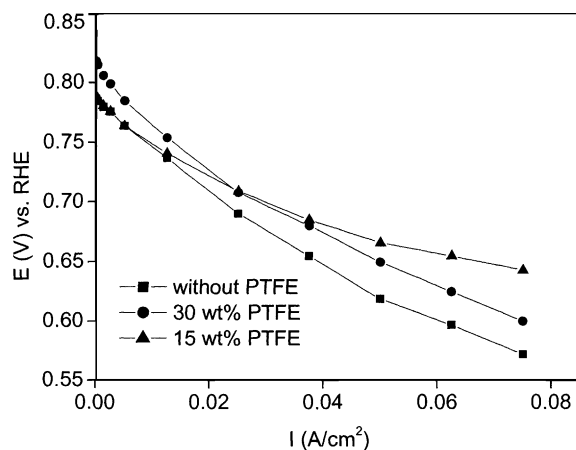


Fig. 6. Effect of PTFE content on cathode performance. Pt loading = 5 mg cm<sup>-2</sup> T = 28 °C; P<sub>O<sub>2</sub></sub>: ambient pressure; O<sub>2</sub> flow rate = 500 ml min<sup>-1</sup>; electrolyte = 2.0 M H<sub>2</sub>SO<sub>4</sub> + 2 M CH<sub>3</sub>OH; electrolyte flow rate = ml min<sup>-1</sup>.

of the cell, which suppresses the favourable effect of PTFE and degrades cell performance.

### 3.4. Effect of amount of PTFE on methanol tolerance

When the electrolyte is 2 M H<sub>2</sub>SO<sub>4</sub> + 2 M CH<sub>3</sub>OH, cathodes containing 15 or 30 wt.% PTFE both gave better performance than cathode without PTFE, as shown in Fig. 6. When operated at a current density of 0.075 A cm<sup>-2</sup>, the φ<sub>c</sub> of the cathode without PTFE is 0.572 and 0.64 V with and without methanol in the electrolyte, respectively as shown in Figs. 5 and 6. Therefore, the difference in φ<sub>c</sub> with and without methanol (denoted as ΔE) is 0.068 V for a cathode without PTFE. The ΔE is 0.06 and 0.007 V for a cathode with 15 and 30 wt.% PTFE, respectively, i.e., values that are smaller than that for a cathode without PTFE, and the ΔE for a cathode with 30 wt.% of PTFE is the smallest. This shows that the PTFE in the cathode catalyst layer acts not only as a hydrophobic agent, but also as a methanol-proof agent. Therefore, addition of an optimum amount of PTFE to the cathode catalyst layer is necessary for increasing the cell performance.

### 3.5. Single-cell performance at various temperatures and methanol concentrations

Polarization curves for a MEA prepared by the sedimentation method at various cell temperatures are presented in Fig. 7. The open-circuit potential of anode (φ<sub>oa</sub>) decreases from 0.24 to 0.18 V when the cell temperature is raised from 40 to 80 °C. This observation is consistent with the results reported by Kuver [22]. Operated at 40 °C and 0.1 A cm<sup>-2</sup>, the overpotential of the anode (denoted as η<sub>a</sub> and η<sub>a</sub> = φ<sub>a</sub> - φ<sub>oa</sub>) is 0.205 V. While the η<sub>a</sub> is only 0.1 and 0.102 V at 60 and 80 °C, respectively. The data in Fig. 7 also show that when the cell is operated at 40 °C, the φ<sub>a</sub> increases by 0.13 V on increasing the current density from 0.1 to 0.125 A cm<sup>-2</sup>.

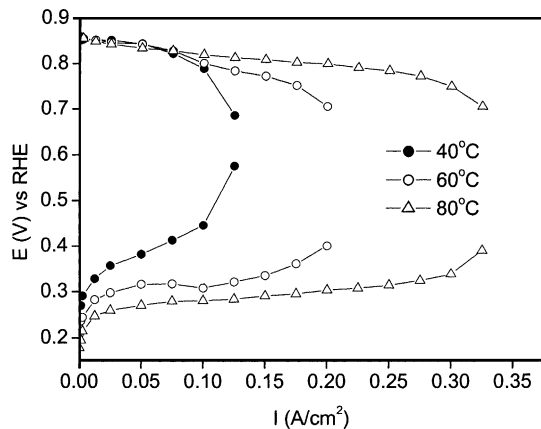


Fig. 7. Current–voltage curves of single-cell cathode and anode at various temperatures. Pt and Pt–Ru loading =  $5 \text{ mg cm}^{-2}$ ;  $P_{\text{O}_2}$ : ambient pressure;  $\text{O}_2$  flow rate =  $500 \text{ ml min}^{-1}$ ;  $\text{CH}_3\text{OH}$ : 2.0 M;  $\text{CH}_3\text{OH}$  flow rate =  $2 \text{ ml min}^{-1}$ .

While at 60 and  $80^\circ\text{C}$ , the  $\varphi_a$  increases by only 0.013 and 0.004 V, respectively. This sharp increase in  $\varphi_a$  at  $40^\circ\text{C}$  is due to the diffusion limit of methanol.

When the cell temperature is increased from 40 to  $80^\circ\text{C}$ , the open-circuit potential of the cathode ( $\varphi_{\text{oc}}$ ) decreases from 0.86 to 0.852 V. Kauranen and Skou [30] have reported that the methanol crossover increases with the increase with cell temperature, which accounts for the decrease in  $\varphi_{\text{oc}}$  observed in this experiment. In addition, an increase of temperature decreases the solubility of oxygen in the water, that is the product of the oxygen reduction reaction (ORR) and is attached to the surface of the catalyst particles in the form of a very thin layer. As the consequence, the access of oxygen to the cathode catalyst sites becomes more difficult as the cell temperature is increased. Simultaneously the catalytic activity of the cathode increases. In the current density range between 0 and  $0.075 \text{ A cm}^{-2}$ ,  $\varphi_c$  changes little with increase in temperature from 40 to  $80^\circ\text{C}$ , due to the fact that the increase of catalytic activity is cancelled by the methanol crossover and the so diffusion limit of oxygen. In the current range from 0.075 to  $0.3 \text{ A cm}^{-2}$ ,  $\varphi_c$  increases with increase in cell temperature, because the increase in catalytic activity now plays a dominant role. At  $40^\circ\text{C}$ ,  $\varphi_c$  decreases by 0.103 V when the current density is raised from 0.1 to  $0.125 \text{ A cm}^{-2}$ . While at 60 and  $80^\circ\text{C}$ ,  $\varphi_c$  decreases by only 0.017 and 0.006 V, respectively. The reason of this rapid decline at  $40^\circ\text{C}$  is that the anode performance decreases rapidly when the current density is increased from 0.1 to  $0.125 \text{ A cm}^{-2}$ , which results in less protons produced and thus the mass-diffusion limit of protons at the cathode side is reached. This phenomenon can also be seen in Fig. 8, which will be discussed later.

Polarization curves for the MEA prepared by the sedimentation method when operated in different methanol solutions are given in Fig. 8. The  $\varphi_{\text{oa}}$  decreases from 0.218 to 0.154 V as the methanol concentration is increased from 1 to 4 M. For 1 M methanol, the  $\varphi_a$  increases sharply from 0.343 to 0.454 V

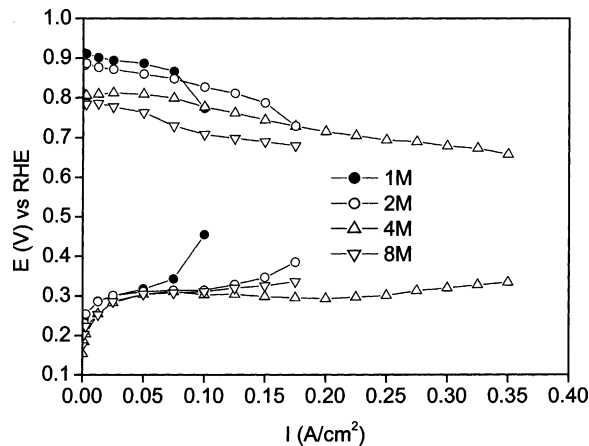


Fig. 8. Current–voltage curves of single-cell cathode and anode operated with various methanol concentrations. Pt and Pt–Ru loading =  $5 \text{ mg cm}^{-2}$ ;  $T = 60^\circ\text{C}$ ;  $P_{\text{O}_2}$ : ambient pressure;  $\text{O}_2$  flow rate =  $500 \text{ ml min}^{-1}$ ;  $\text{CH}_3\text{OH}$ : 2.0 M;  $\text{CH}_3\text{OH}$  flow rate:  $2 \text{ ml min}^{-1}$ .

when the current is raised from 0.075 to  $0.1 \text{ A cm}^{-2}$ , due to the mass-transportation limit at low methanol concentration. At a current density of  $0.05 \text{ A cm}^{-2}$ , the  $\varphi_a$  is 0.304, 0.301 and 0.308 V when the methanol concentration is 2, 4 and 8 M, respectively. Clearly, there is no great difference in  $\varphi_a$ . As the current density is further increased to  $0.15 \text{ A cm}^{-2}$ , however, the  $\varphi_a$  is 0.347, 0.298 and 0.325 V, for 2, 4 and 8 M methanol, respectively. Therefore, the optimum methanol concentration is 4 M. In this solution, the  $\varphi_a$  increases by only 0.033 V when the current density is increased from 0.05 to  $0.35 \text{ A cm}^{-2}$  which means that mass transportation is less of a problem at the anode side.

The cathode performance is also affected markedly by the methanol concentrations due to the crossover of methanol. The  $\varphi_{\text{oc}}$  decreases from 0.91 to 0.81 V as the methanol concentration is increased from 1 to 4 M due to the formation of a mixed potential of oxygen and methanol at the cathode. With a methanol concentration of 1 M, the  $\varphi_c$  decreases sharply from 0.867 to 0.773 V when the current is increased from 0.075 to  $0.1 \text{ A cm}^{-2}$ . At this current density, a sharp decrease of anode performance is also observed, as discussed previously. Therefore, this sharp decrease in cathode performance is due to the mass-transportation limit of protons at the cathode, which was caused by the insufficient protons generated by the anode. At 4 M methanol, no steep decline in  $\varphi_c$  is observed, even for a current density of  $0.35 \text{ A cm}^{-2}$ . An increase in methanol to 8 M causes a further degradation in cathode performance. As shown in Figs. 8 and 9, when the current density is less than  $0.075 \text{ A cm}^{-2}$ , the cathode performance plays a dominant role in cell performance, which decreases with increase in methanol concentration. Above  $0.075 \text{ A cm}^{-2}$ , however both the anode and the cathode influence the cell performance. Therefore, methanol crossover and methanol tolerance of the cathode are prominent problems in a micro DMFC, which in most circumstances operates under a relatively small current load.

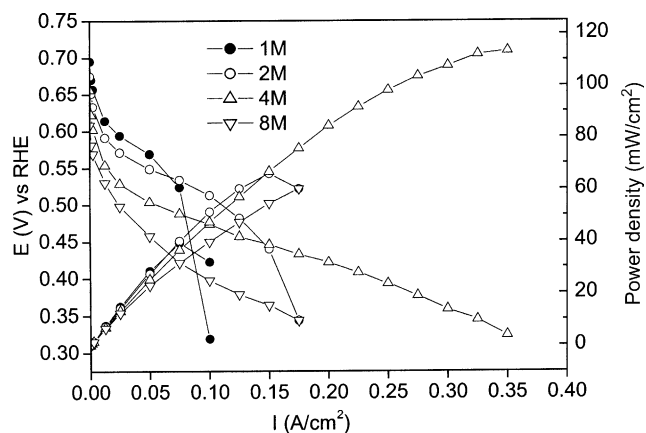


Fig. 9. Power density curves of single cell operated with various methanol concentrations. Pt and Pt–Ru loading =  $5 \text{ mg cm}^{-2}$ ;  $T = 60^\circ\text{C}$ ;  $P_{\text{O}_2}$ : ambient pressure;  $\text{O}_2$  flow rate =  $500 \text{ ml min}^{-1}$ ;  $\text{CH}_3\text{OH} = 2.0 \text{ M}$ ;  $\text{CH}_3\text{OH}$  flow rate =  $2 \text{ ml min}^{-1}$ .

The power density curves (Fig. 9) show that the peak value appears at a cell voltage of 0.524 V when the methanol concentration is 1 M, due to the rapid deterioration of cell performance at  $0.1 \text{ A cm}^{-2}$ . When the methanol concentration is 4 M, the power density does not reach a peak value, even at a cell voltage of 0.33 V. Operated at 0.4 V, the power density is  $92 \text{ mW cm}^{-2}$ . This value is 64% higher than the power density obtained with 2 M methanol, which is the solution adopted by most workers. Thus, the fewer pinholes and the reduced thickness of the MEA prepared by the sedimentation method enhances the tolerance towards methanol.

#### 4. Conclusions

A DMFC electrode is prepared by the sedimentation method. Reducing the manual work to the minimum, this method greatly decreases the systematic errors and a planar and homogeneous catalyst layer is produced. Operating at  $60^\circ\text{C}$ , the power density of such a MEA is 70% higher than that prepared by a conventional brushing method. The preparation process and the operating conditions have been optimized. Using an impregnation method to introduce Nafion into the catalyst layer, the MEA prepared by the sedimentation method fields better performance. It is found that the addition of PTFE to the cathode catalyst layer increases the tolerance of the cathode to methanol. The optimum methanol concentration is 4 M.

#### Acknowledgement

This research was funded by CUPS sponsored by KOSEF and the BK 21 fund (2003–2004).

#### References

- [1] A.S. Arico, P. Creti, H. Kim, R. Mantegna, N. Giordano, V. Antonucci, *J. Electrochem. Soc.* 143 (1996) 3950.
- [2] D.H. Jung, C.H. Lee, C.S. Kim, D.R. Shin, *J. Power Sources* 71 (1998) 169.
- [3] S. Wasmus, A. Kuver, *J. Electroanal. Chem.* 461 (1999) 14.
- [4] B.D. McNicol, D.A.J. Rand, K.R. Williams, *J. Power Sources* 83 (1999) 15.
- [5] M. Baldauf, W. Preidel, *J. Power Sources* 84 (1999) 161.
- [6] B.D. McNicol, D.A.J. Rand, K.R. Williams, *J. Power Sources* 100 (2001) 47.
- [7] A.S. Arico, S. Srinivasan, A. Antonucci, *Fuel Cells* 1 (2001) 133.
- [8] C. Lamy, A. Lima, V. LeRhun, F. Delime, C. Coutanceau, J.-M. Leger, *J. Power Sources* 105 (2002) 283.
- [9] Z. Siroma, N. Fujiwara, T. Ioroi, S. Yamazaki, K. Yasuda, Y. Miyazaki, *J. Power Sources* 126 (2004) 41.
- [10] Rongzhong Jiang, Charles Rong, Deryn Chu, *J. Power Sources* 126 (2004) 119.
- [11] W.C. Choi, J.D. Kim, S.I. Woo, *Catal. Today* 74 (2002) 235.
- [12] K.-W. Park, H.-J. Ahn, Y.-E. Sung, *J. Power Sources* 109 (2002) 500.
- [13] E.M. Crabb, M.K. Ravikumar, *Electrochim. Acta* 46 (2001) 1033.
- [14] C.S. Kim, Y.G. Chun, D.H. Peck, D.R. Shin, *Int. J. Hydrogen Energy* 23 (1998) 1045.
- [15] L.J. Hobson, Y. Nakano, H. Ozu, S. Hayase, *J. Power Sources* 104 (2002) 79.
- [16] D. Bevers, N. Wagner, von Bradke, S. M., *Int. J. Hydrogen Energy* 23 (1998) 57.
- [17] K. Bolwin, E. Gulzow, D. Bevers, W. Schnurnberger, *Solid State Ionics* 77 (1995) 324.
- [18] Y.G. Chun, C.S. Kim, D.H. Peck, D.R. Shin, *J. Power Sources* 71 (1998) 174.
- [19] C.K. Subramanian, N. Rajalakshmi, K. Ramya, K.S. Dhathathreyan, *Bull. Electrochem.* 16 (2000) 350.
- [20] S. Moller-Holst, *Denki Kagaku* 64 (1996) 699.
- [21] M.S. Wilson, S. Gottesfeld, *J. Appl. Electrochem.* 22 (1992) 1.
- [22] A. Kuver, W. Vielstich, *J. Power Sources* 74 (1998) 211.
- [23] W.C. Choi, J.D. Kim, S.I. Woo, *J. Power Sources* 96 (2001) 411.
- [24] A.K. Shukla, R.K. Raman, N.A. Choudhury, K.R. Priolkar, P.R. Sarode, S. Emura, R. Kumashiro, *J. Electroanal. Chem.* 563 (2004) 181.
- [25] B. Yang, A. Manthiram, *Electrochem. Commun.* 6 (2004) 231.
- [26] G.Q. Sun, J.T. Wang, R.F. Savinell, *J. Appl. Electrochem.* 28 (1998) 1087.
- [27] S. Wasmus, A. Kuver, *J. Electroanal. Chem.* 461 (1999) 14.
- [28] M. Waidhas, W. Drenckhahn, W. Preidel, H. Landes, *J. Power Sources* 61 (1996) 91.
- [29] A.K. Sukla, P.A. Christensen, A.J. Dickinson, A. Hamnett, *J. Power Sources* 76 (1998) 54.
- [30] S. Kauranen, E. Skou, *J. Appl. Electrochem.* 26 (1996) 909.